



Glucose dehydration to 5-hydroxymethylfurfural over phosphate catalysts

V.V. Ordonsky^a, V.L. Sushkevich^b, J.C. Schouten^a, J. van der Schaaf^a, T.A. Nijhuis^{a,*}

^aLaboratory of Chemical Reactor Engineering, Eindhoven University of Technology, P.O. Box 513, 5600 MB Eindhoven, The Netherlands

^bDepartment of Chemistry, Moscow State University, Leninskye Gory 1/3, 119991 Moscow, Russia

ARTICLE INFO

Article history:

Received 3 October 2012

Revised 26 November 2012

Accepted 23 December 2012

Available online 1 February 2013

Keywords:

Glucose
Dehydration
HMF
Phosphates

ABSTRACT

Glucose dehydration has been studied over aluminum (AlPO), titanium (TiPO), zirconium (ZrPO), and niobium phosphates (NbPO). The experimental results suggest that the activity of glucose transformation decreases in the order: NbPO > ZrPO > TiPO > AlPO, which was determined to correspond to the amount of strong acid sites on these catalysts. The selectivity to 5-hydroxymethylfurfural (HMF) varies in the range of 30–60% and depends on the ratio of Brønsted to Lewis acid sites. Excess of Lewis acidity on the catalyst leads to unselective glucose transformation into humins. Modification of the catalysts by a silylation procedure or by deeper treatment with phosphoric acid leads to drastic increase in the selectivity to HMF due to the deactivation of unselective Lewis acid sites. It is proposed that a synergism of a protonated phosphate group and a nearby metal Lewis acid site in the two-stage glucose transformation into HMF leads to a highly selective glucose dehydration.

© 2013 Elsevier Inc. All rights reserved.

1. Introduction

Over the last years, the dehydration of carbohydrates to 5-hydroxymethylfurfural (HMF) has attracted increasing attention due to its possible application as a substitute for petroleum based building blocks [1]. HMF and its derivatives can be applied as platform chemicals, precursor for polymers, fuels, or solvents [2].

Fructose dehydration to HMF is easy to realize over homogeneous and heterogeneous acidic catalysts in aqueous or organic phase [3,4], multiphase systems [5], and ionic liquids [6]. The low availability and high price of fructose in comparison with glucose, which is the main building block of biomass, increase interest in the methods for effective glucose dehydration to HMF. Unfortunately, glucose as an aldohexose leads to low HMF selectivity in the direct dehydration due to side reactions like cross-condensation with formation of humins.

The most popular method of glucose dehydration to HMF at the moment is based on the application of metal halides like CrCl₂ in different ionic liquids or organic solvents [7,8]. The catalyst promotes the isomerization of glucose to fructose followed by a dehydration to HMF. A combination of acidic and basic heterogeneous catalysts like Amberlyst-15 and hydrotalcite in the presence of aprotic organic solvents also gives high yields of HMF [9]. However, the application of ionic liquids and high boiling solvents results in a significant increase in the price of the process due to difficult separation and purification stages. It would be preferable to use water in the dehydration process. At the moment, in literature heterogeneous

catalysts for HMF production demonstrate a low HMF yield and require a high reaction temperature.

Glucose dehydration over zirconia and titania oxides by Watanabe et al. [10] resulted in a yield of HMF lower than 30% at 200 °C. Yan [11] used sulfated zirconia for glucose dehydration to HMF with a 36% yield at 200 °C. The most promising systems for glucose dehydration to HMF were shown to be niobic acid and tantalum hydroxides treated with phosphoric [12,13]. The yield of HMF was close to 50% in a biphasic system of water-2-butanol at 160 °C.

The main reason for the unselective process of glucose transformation over heterogeneous catalysts in our point of view lies in unbalanced functions of isomerization of glucose into fructose and dehydration of fructose into HMF. This leads to a requirement for more severe conditions for the reaction and unselective condensation of sugars into humins.

In this work, we studied the role of the type and amount of Lewis and Brønsted acid sites in glucose transformation over different phosphates. The strength of the acid sites was varied by application of different metals in the row Al, Ti, Zr, and Nb. The Lewis acidity of phosphates was modified by silylation with tetraethoxysilane (TEOS).

2. Experimental

2.1. Catalysts

Aluminum, titanium, zirconium, and niobium phosphates were prepared using different procedures described in literature [14–17]. Aluminum phosphate (AlPO) was prepared by the addition of aqueous ammonia (25 wt.%) to an aqueous solution

* Corresponding author.

E-mail address: t.a.nijhuis@tue.nl (T.A. Nijhuis).

containing equimolar quantities of aluminum chloride and orthophosphoric acid (1 M) until a pH 7.0 was reached [14]. Titanium phosphate (TiPO) was prepared by a fast addition of an aqueous solution of TiCl_4 (7.5 g) in 1 M HCl (20 mL) to orthophosphoric acid (5.92 g in 20 mL water) while intensively stirring [15]. Phosphoric acid (23.3 g) in water (470 mL) was added quickly to a rapidly stirred solution of zirconyl chloride (22.5 g) in water (140 mL) at ambient temperature (ZrPO) [16]. Niobium phosphate (NbPO) was synthesized by a treatment of hydrated niobium oxide provided by CBMM in Brazil (5 g) with diluted orthophosphoric acid (9 g in 160 mL of H_2O) at 70 °C for 7 h [17]. NbPO-f was synthesized by the same treatment of the fresh niobium oxide. The fresh niobium oxide was prepared by preliminary fusion of niobium oxide with KOH by gradually heating up to 450 °C, dissolution in hot water, and precipitation by addition of nitric acid. The resulting phosphates were aged at ambient temperature and then filtered and washed with a large amount of water. The solid was dried (100 °C) and calcined at 400 °C for 3 h in a flow of air.

Na/NbPO-f and Na/ZrPO were prepared by threefold ion exchange of NbPO-f and ZrPO at 50 °C with 1 M solution of sodium carbonate.

Aluminum, titanium, and zirconium oxides were prepared by similar methods. Aluminum (Al_2O_3), titanium (TiO_2), and zirconium (ZrO_2) oxides were prepared by the addition of aqueous ammonia (25 wt.%) to an aqueous solution of chlorides. Niobium oxide (Nb_2O_5) was used from the described procedure for the preparation of NbPO-f. The resulting oxides were aged at ambient temperature and then filtered and washed with a large amount of water. The solid was dried (100 °C) and calcined at 400 °C for 3 h in a flow of air.

The surface modified samples ZrPO/Si, NbPO/Si, and Nb_2O_5 /Si were prepared by the chemical liquid deposition of silica over ZrPO, NbPO, and Nb_2O_5 , respectively, using TEOS as the silylation agent. 4 g of dried catalysts were added to a solution of 1 g of TEOS in 100 mL of n-hexane. The mixture was stirred at 50 °C for 24 h. The samples were subsequently washed with water and dried.

2.2. Characterization

The chemical composition of the samples was determined by inductively coupled plasma (ICP) spectroscopy. All measurements were performed on an ELAN ICP-MS machine (Perkin Elmer). Prior to the measurements, the exact amount of catalyst (~100 mg) was dissolved in 0.4 g of concentrated hydrofluoric acid (40%). This solution was diluted by distilled water to obtain a concentration of measured ions of about 1 mg/L. Solutions for calibration were prepared from the standards with addition of the corresponding amount of HF to level the matrix effect. Sorption-desorption isotherms of nitrogen were measured using an automated porosimeter (Micrometrics ASAP 2000). Prior to the measurements, the samples were evacuated at 300 °C. The XRD patterns were recorded with a DRON-3M diffractometer, applying Cu K α radiation. The acidic properties were studied by temperature-programmed desorption of ammonia (NH_3 TPD). Prior to adsorption, the samples were calcined in situ in a flow of dry air at 400 °C for 1 h and, subsequently, in a flow of dry helium for 1 h and cooled down to ambient temperature. For NH_3 adsorption, a sample was subjected to a flow of diluted NH_3 for 30 min at ambient temperature. The physisorbed NH_3 was removed in a flow of dry He at 100 °C for 1 h. Typical TPD experiments were carried out in the temperature range of 100–800 °C in a flow of dry He. The rate of heating was 7 °C/min. The desorbed NH_3 was analyzed by a thermal conductivity detector (TCD) detector. The water formed during desorption at high temperatures was trapped using a cold trap.

IR spectra were recorded with a Nicolet Protégé 460 FT-IR spectrometer with 4 cm^{-1} optical resolution. Prior to the measurements,

the catalysts were pressed in self-supporting disks and activated in the IR cell attached to a vacuum line at 300 °C for 4 h. Adsorption of pyridine (Py) was performed at 150 °C for 30 min. The excess of Py was further evacuated at 150 °C for 1 h. The adsorption–evacuation was repeated several times until no changes in the spectra were observed.

^{31}P solid-state NMR was performed using a Bruker Avance-400 spectrometer.

Adsorption of glucose or fructose on the catalysts was studied by addition of 1 g of catalyst to a solution of 1.85 mmol of glucose or fructose in 10 mL of water. The mixture was stirred for 0.5 h at 298 K. The amount of adsorbed glucose or fructose was determined using HPLC (Shimadzu) equipped with refractive index detector by determining the remaining concentration in the water.

2.3. Sugars dehydration

Experiments were carried out in a 100-mL stirred autoclave working in a batch mode. The procedure for testing catalysts was as follows: catalyst (2 g) and water (40 mL) were poured into the autoclave. Methylisobutylketone (MIBK) or 2-methyltetrahydrofuran (MTHF) was added to the autoclave in the experiments with solvent. The autoclave was purged with nitrogen. Fructose or glucose (4 g) dissolved in 20 mL of water was forced into the autoclave from a storage vessel by high-pressure N_2 after the temperature had been increased to 135 °C, after which the catalytic experiment was started. The agitation speed was 500 rpm.

Periodically, liquid samples were taken from the autoclave, which were analyzed using HPLC (Shimadzu) equipped with refractive index and UV-Vis detectors with a BIO-RAD Aminex HPX-87H column.

Reactant conversion and product selectivity was defined as follows:

$$\text{Conversion (mol.\%)} = \frac{\text{(moles of fructose or glucose reacted)}}{\text{(moles of initial fructose or glucose)}} \cdot 100\%$$

$$\text{Selectivity (mol.\%)} = \frac{\text{(moles of produced HMF, fructose, glucose or levulinic acid)}}{\text{(moles of fructose or glucose reacted)}} \cdot 100\%$$

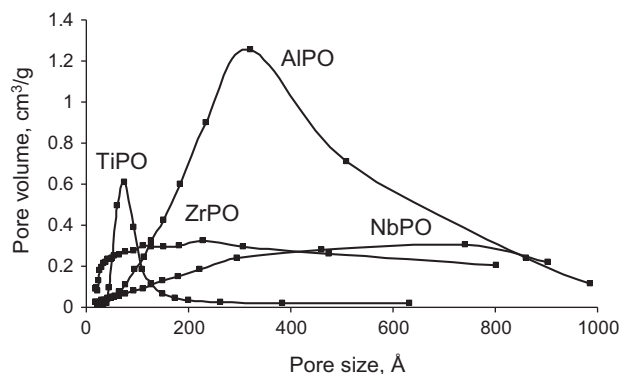
3. Results and discussion

3.1. Physico-chemical properties of catalysts

The properties of the catalysts are given in Table 1. All studied catalysts show XRD patterns typical for an amorphous material (not shown). Nitrogen adsorption data indicate that the amorphous phosphates have a high surface area with a very broad distribution of pore sizes (Fig. 1). Sizes of the pores for phosphates are higher than 100 Å, except for TiPO that has narrow pore size distribution in the range 50–120 Å. The amorphous phosphates have completely different M/P molar ratios, which is due to the different ways of their preparation. They are most probably composed of a mixture of phosphates, polyphosphates, and hydrophosphates with different M/P ratios. The ZrPO catalyst has the highest content of phosphorus, which can be explained by the formation of a layered structure with bridged phosphate groups between layers [18]. The lowest content of phosphorus has the NbPO sample due to the incomplete transformation of niobium oxide into phosphate [16,17]. Indeed, in this case, only a niobium oxide surface area is exposed to interaction with phosphoric acid in comparison with the direct mixing of chlorides with phosphoric acid. All the attempts to increase the phosphorus content in the sample NbPO

Table 1
Characterization of catalysts.

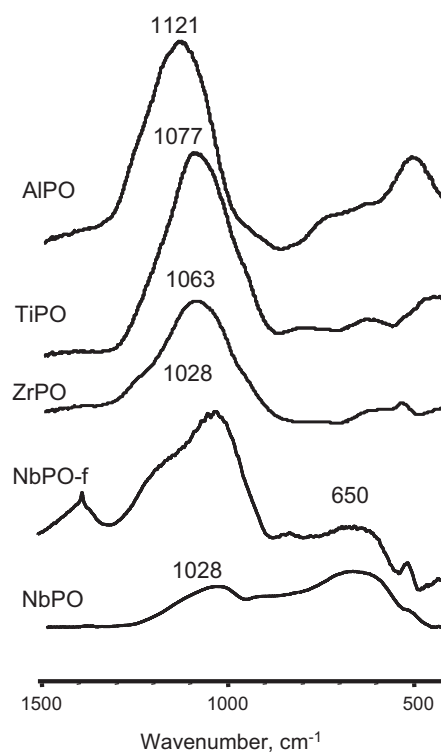
Catalyst	Elemental analysis		Surface area, (m ² /g)	TPD NH ₃ (μmol/g)	Py adsorption (μmol/g)			Adsorption (μmol/g)	
	M/P	Na/P			Brønsted (B)	Lewis (L)	B/L	Fructose	Glucose
AlPO	1.1	0	140	1097	90	950	0.09	1.2	0
TiPO	0.9	0	80	762	300	470	0.64	7.6	0.6
ZrPO	0.6	0	210	1725	280	1440	0.19	39.2	5.5
Na–ZrPO	0.6	0.6	210	–	20	1340	0.01	–	–
ZrPO/Si	0.6	0	210	–	272	620	0.44	20.7	1.1
NbPO	4.1	0	67	345	75	280	0.27	17.2	2.4
NbPO-f	2.4	0	70	736	370	370	1.00	10.5	0.2
Na/NbPO-f	2.4	0.8	70	–	0	90	0.00	–	–

**Fig. 1.** Pore size distribution in the phosphate catalysts.

by using a higher concentration of orthophosphoric acid or higher temperature lead to drastic loss of the surface area of the catalyst due to crystallization of the material. Low amount of surface hydroxyl groups over niobium oxide leads to a low amount of formed phosphate groups (Table 1). In order to increase the amount of hydroxyl groups over niobium oxide, it was transformed into potassium niobate with subsequent dissolution in water and precipitation by addition of nitric acid into fresh niobium acid. This activation procedure led to significant increase in the amount of phosphate groups in NbPO-f after treatment of fresh niobium acid with phosphoric acid (Table 1). The ratio Nb/P decreased from 4.1 to 2.4.

The IR spectra of the phosphates are shown in Fig. 2. A broad band in the range of 1000–1200 cm⁻¹ can be assigned to O=P=O asymmetric stretching vibrations of phosphate or polyphosphate species [19]. This band shifts from 1121 cm⁻¹ for AlPO to 1028 cm⁻¹ for NbPO. This effect is in line with the decreasing electronegativity of the metals and the simultaneous increase in the ionic character of the bond between metal and phosphate species in the order: Al < Ti < Zr < Nb. The band at 650 cm⁻¹ for niobium phosphates is attributed to a skeletal vibration previously reported for amorphous niobium acid [19,20]. The high M/P ratio for niobium phosphate indicates a large quantity of metal oxide phase. For the sample NbPO-f, the modification of the fresh niobium acid leads to a significant increase in the intensity of the phosphate band and a decrease in the contribution of niobium oxide (Fig. 2).

The state of phosphate groups in phosphates has been studied by the solid-state ³¹P magic-angle-spinning NMR. The spectra of ZrPO, TiPO, and AlPO are presented in Fig. 3. Niobium phosphate was not included because of the very broad peak, which might be explained by a wide variation in coordination of the phosphate groups. All spectra exhibit the main peak in the range of –24 to –26 ppm. The increase in the chemical shift for AlPO to –24.5 ppm in comparison with ZrPO and TiPO is the result of an increase in the electronegativity of the metal and electron density over P [21]. Apart from the main peak, ZrPO has additional shoulders at –12 and

**Fig. 2.** FTIR spectra in the region of structural stretching vibrations of phosphates.

–20.6 ppm. It was shown earlier that the chemical shift ³¹P depends on the amount of Zr atoms attached to P [22,23]. The higher amount of bonds of P with the metal the higher will be the shift towards higher magnetic field. Thus, the main peak in phosphates might be attributed to the formation of three coordinated phosphate (Zr–O)₃P(OH)₂. Lines at –20.6 and –12 ppm in ZrPO correspond to formation of (Zr–O)₂PO(OH) and (Zr–O)PO(OH)₂. Appearance of ³¹P corresponding to low interaction with Zr indicates the presence of interlayer phosphate species. Similar lines were observed over α-zirconium phosphate with the P/Zr ratio 2 [23]. This explains the low Zr/P ratio in ZrPO. Formation of polyphosphates should be observed by the appearance of lines in the range –35 to –45 ppm [23], but these lines were not observed in the spectrum (Fig. 3).

The ion exchange of NbPO-f or ZrPO samples does not lead to any changes of the Nb/P or Zr/P molar ratios (Table 1). Therefore, we can assume that the ion exchanged materials preserve the structure of parent phosphates. The content of sodium introduced is given in Table 1. The results show that ion exchange with sodium carbonate leads to a deep substitution of the acidic protons with sodium cations.

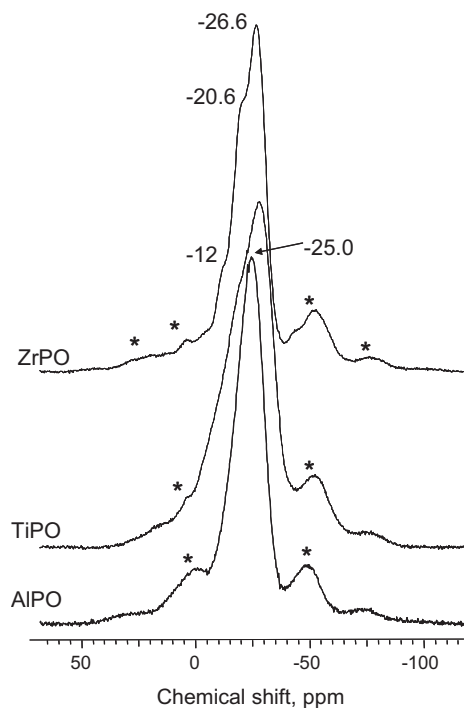


Fig. 3. ^{31}P -NMR spectra of AlPO, ZrPO, and NbPO. * Spinning side bands.

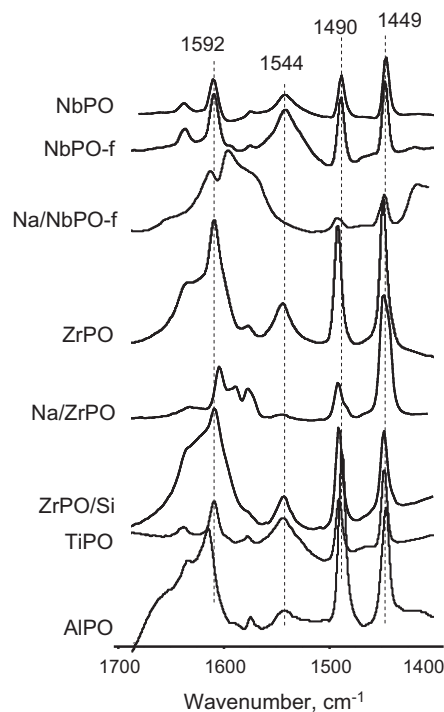


Fig. 5. FTIR spectra of pyridine adsorbed over phosphates.

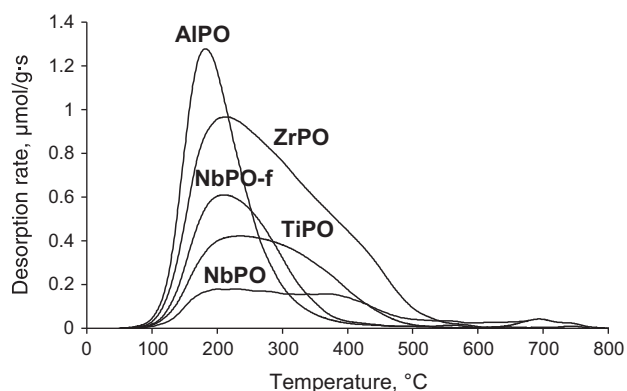


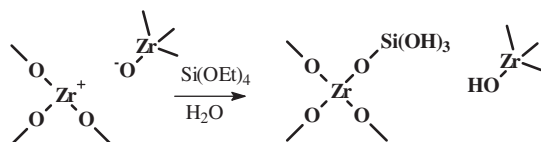
Fig. 4. TPD- NH_3 profiles.

The amount and strength of the acid sites of phosphate catalysts have been studied by temperature-programmed desorption of ammonia (Fig. 4). The strength of acid sites and the temperature of NH_3 desorption should increase according to the increase in the ionic character in the row $\text{Al} < \text{Ti} < \text{Zr} < \text{Nb}$. The TPD- NH_3 profiles show one peak in the temperature range of 100–500 °C for all the samples studied. For NbPO-f and AlPO, this peak is rather narrow and is shifted to lower temperature, which points to acid sites with medium strength. Differently, NbPO, TiPO, and ZrPO desorb ammonia over a wide range of temperatures from 100 to 500 °C, which corresponds to the medium and the strong acid sites. The total amount of the acid sites determined by TPD- NH_3 correlate with the surface area of samples (Table 1). The broad peaks of ammonia desorption over phosphates which do not correspond with the row of electronegativity are the result of the higher heat of adsorption of ammonia over Lewis acid sites compared to that over Brönsted acid sites [24]. This results in desorption of ammonia with a broad distribution of energies from different types of Lewis acid sites.

The nature of the acid sites was studied by IR spectroscopy of adsorbed pyridine, and the IR spectra are shown in Fig. 5. The main bands observed for all the samples can be assigned according to the literature data [25,26]: the bands at 1592 and 1490 cm^{-1} are due to H-bonded pyridine, the band at 1544 cm^{-1} is attributed to pyridine protonated on Brönsted sites, and the band at 1449 cm^{-1} is assigned to pyridine adsorbed on Lewis acid sites.

Table 1 gives the concentration of the Brönsted and Lewis acid sites calculated on the basis of the extinction coefficients for bands at 1545 and 1454 cm^{-1} [27]. The intensity of the band assigned to pyridine adsorbed on Brönsted acid sites increases in the following order: AlPO \approx NbPO $<$ TiPO \approx ZrPO (Fig. 5) and correlates mainly with the ionic character of the bond. Other factors like the amount of phosphate groups and the surface area also influence the concentration of Brönsted acid sites. Indeed, the low adsorption of pyridine over niobium phosphate is the result of low amount of phosphate groups in NbPO (Table 1). Treatment of fresh niobic acid with phosphoric acid (NbPO-f) leads to a significant increase in the amount of Brönsted acid sites and decrease in the contribution of the Lewis acidity in accordance with the higher amount of phosphate groups in this sample (Fig. 5, Table 1). The higher surface area of ZrPO in comparison with other phosphates does not result in an increase in the concentration of Brönsted acid sites, even though the Lewis acidity is significantly higher. This might be explained by the presence of phosphate groups in ZrPO with a lower coordination with Zr atoms (Fig. 3), which might result in a lower acidity of phosphate groups and a high Lewis acidity. The results show that the amount of Brönsted acid sites is lower than the amount of Lewis acid sites for all phosphates. Lewis acidity determined by Py does not correlate with the electronegativity of metals but correlates with the amount of desorbed ammonia and reflects also the high binding energies of Py with Lewis acid sites (Table 1).

The decrease in the excess of Lewis acid sites in zirconium phosphate was realized by treatment of the catalyst with TEOS. This procedure is well known for deactivation of acid sites on the external surface of zeolites [28] but was not applied yet for modification of phosphates. The modification does not lead to any changes in



Scheme 1.

the texture of the catalyst, which can be observed by similar results in the nitrogen adsorption (Table 1). Treatment of zirconium phosphate with TEOS leads mainly to a deactivation of the Lewis acidity with a low effect on the Brönsted acid sites (Fig. 5, Table 1). This fact might be explained by a low stability and easy hydrolysis of the Si—O—P bonds in comparison with Si—O—Al bonds. Lewis acid sites in phosphates can be divided into two groups: Lewis acid sites formed by metal attached to the phosphate group (—Zr—O—P—) [29] and Lewis acid sites formed by coordinatively unsaturated metal ions like in oxides [30]. Treatment of the catalyst with TEOS might lead to a hydrolysis of TEOS on unsaturated metal sites with the formation of Si—O—Zr bonds and a deactivation of this type of Lewis acid sites (Scheme 1). The first type of the Lewis acidity in Zr—O—P groups should be less affected by the treatment with TEOS due to the saturated metal.

The presence of the Lewis acid sites bound with a phosphate group might be observed by catalyst treatment with Na_2CO_3 . Treatment of NbPO-f with Na_2CO_3 leads to a disappearance of Brönsted acid sites (Fig. 5). At the same time, the intensity of the peak at 1449 cm^{-1} , attributed to Py adsorption over Lewis acid sites, also significantly decreased. This observation might be explained by

changes in the electronic state of the Lewis acid site after exchange of a nearby proton with Na^+ . Protons compete with metal Lewis sites for electrons of oxygen. Ion exchange with Na^+ should lead to a decrease in the positive charge over Nb and strength of the Lewis acid site. The effect of ion exchange with alkali metal on the spectra of Py adsorption over Lewis acid sites provides information on the proximity of Brönsted and Lewis acid sites on the catalyst NbPO-f. The influence of the strength that coexisting Brönsted and Lewis acid sites have on each other was shown earlier in the literature [31].

At the same time, adsorption of Py over Na/ZrPO shows that the elimination of protons does not lead to a significant decrease in the amount of Lewis acid sites (Fig. 5, Table 1). This observation might be explained by a high amount of unsaturated Lewis acid sites isolated from phosphate groups. Ion exchange with Na^+ should not significantly affect the amount and strength of Lewis acid sites in this case.

To summarize, our results suggest that the amount of strong Brönsted acid sites increases in accordance with the decrease in the electronegativity of the metals. Lewis acidity in phosphates consists of metal sites bound to phosphate groups and isolated coordinatively unsaturated sites. Treatment of phosphates with TEOS results in a decrease in the amount of isolated Lewis acid sites.

3.2. Dehydration of sugars

3.2.1. Glucose dehydration over phosphates

The conversion of glucose and the selectivity to HMF, fructose, and levulinic acid during dehydration of glucose over the different

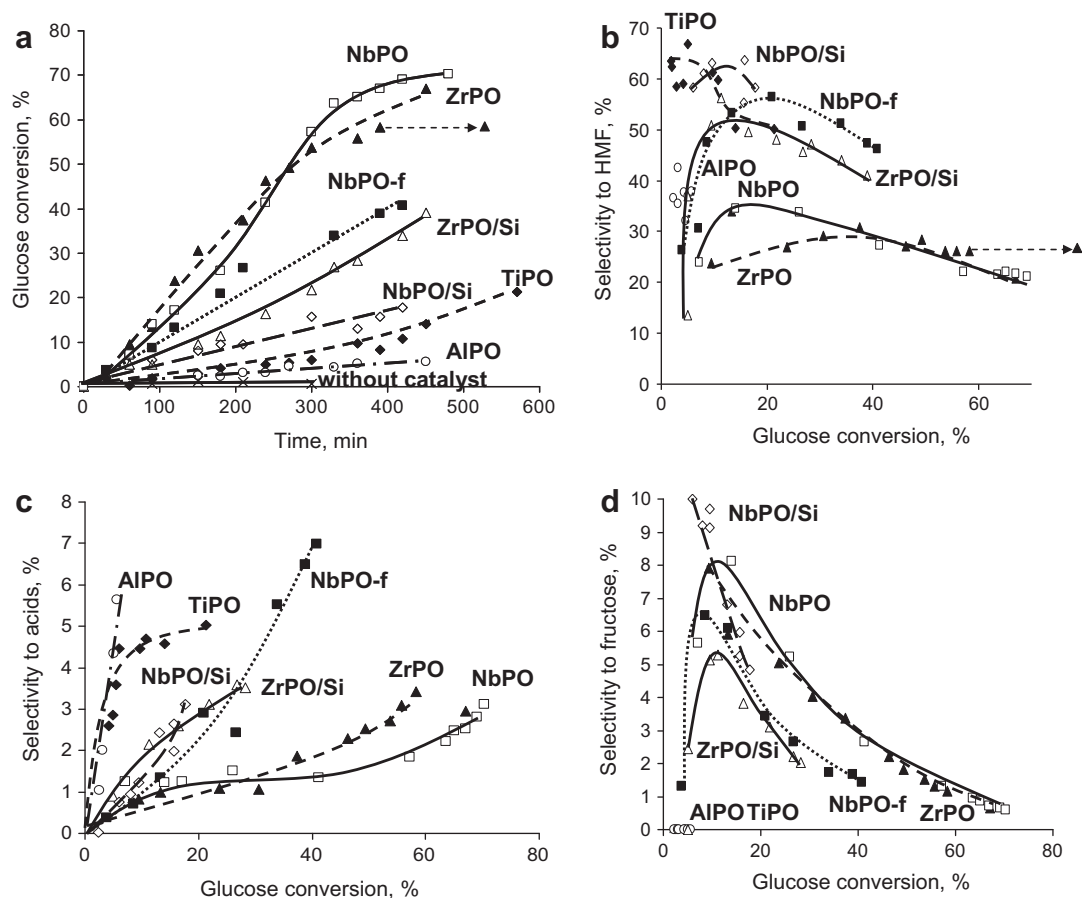


Fig. 6. Glucose conversion versus time (a), selectivity to HMF (b), selectivity to acids (c), and fructose (d) versus glucose conversion over phosphates. Dotted arrows show results of the experiment after filtering of ZrPO and heating of the solution for an additional 2 h.

catalysts are shown in Fig. 6. Besides, these main products furfural was detected in the reaction system by HPLC. The selectivity to furfural did not exceed 1 mol.%, and therefore, we did not investigate its formation further. The appearance of furfural was explained previously by a fast reverse-aldol cleavage of carbohydrates [32]. Formic and levulinic acids are the products of HMF rehydration over acidic catalysts [33]. The main side reaction is the formation of polymeric humins by condensation of HMF and sugars [34]. Humins could not be observed by HPLC, and their amount was calculated from the carbon balance.

The results of the reaction without addition of catalyst (Fig. 6a) show that the conversion of glucose is lower than 1% indicating a high stability of glucose at this temperature. Activity of the parent phosphates in the glucose transformation increases in the order: $\text{AlPO} < \text{TiPO} < \text{ZrPO} \approx \text{NbPO}$. This order corresponds to the decrease in electronegativity of the metals and the increase in the ionic character between the metal and the phosphate group. It provided information on the role of the strength of the acid sites in the glucose dehydration to HMF. The total acidity of the phosphates determined by TPD of NH_3 does not correlate with the activity of the catalysts (Fig. 4). A similar trend in the activity for this type of catalysts was observed during the Prins condensation of formaldehyde with isobutene over phosphates [35].

The selectivities to HMF over phosphates have bell-shaped curves (Fig. 6b). This form might be explained by an initial interaction of glucose with the surface of the catalyst and a decrease in the selectivity to HMF at high conversions, due to secondary HMF transformation by rehydration of HMF into formic and levulinic acids and secondary condensation of HMF into humins [34]. The selectivity to HMF for TiPO is close to 50% at 20% conversion of glucose. At the same time, the maximum selectivity to HMF for niobium (NbPO) and aluminum phosphate (AlPO) is near 35% and for zirconium phosphate it is even lower (30%).

The presence of a homogeneous catalyst due to the leaching of phosphate and metal species could be the reason of the low selectivity of the glucose dehydration over phosphates. In order to probe this hypothesis in the experiment over ZrPO, the catalyst was removed by filtration after 6.5 h of the reaction. The filtrate was subsequently allowed to react at the same temperature for a further 2 h. The results show (Fig. 6) that the reaction did not continue once the catalyst was removed and the selectivity to HMF did not change, indicating that no homogenous catalysis occurred by leached metal and phosphate ions.

The selectivity to formic and levulinic acid is shown in Fig. 6c. The high selectivity of AlPO and TiPO to acids is the result of the rehydration of HMF, which is more significant when the catalyst has a low activity in the dehydration of the more stable glucose molecule. The selectivity to acids over NbPO and ZrPO slowly increases till 2–3% at 60% conversion of glucose.

The dehydration of glucose to HMF, as was shown earlier over different Lewis acidic systems, contains two stages: isomerization of glucose to fructose and fructose dehydration to HMF [36,37]. Glucose isomerization to fructose is very significant in the initial stage of the reaction over ZrPO and NbPO (Fig. 6d). The selectivity to fructose increases fast to 8% at a low conversion of glucose and decreases during the reaction to 1%. At the same time, AlPO and TiPO do not show the formation of fructose. This is the result of the weak Lewis acid sites of these catalysts, which are not active in the isomerization of glucose. The formation of a small amount of fructose in this case should be accompanied by a fast dehydration to HMF. At the same time, the high amount of formed fructose in the case of NbPO and ZrPO might be responsible for the low selectivity to HMF due to the unselective fructose dehydration to HMF over Lewis acid sites [34].

Summation of the selectivity of all detected products like HMF, acids, and fructose show that approximately 50% of glucose is

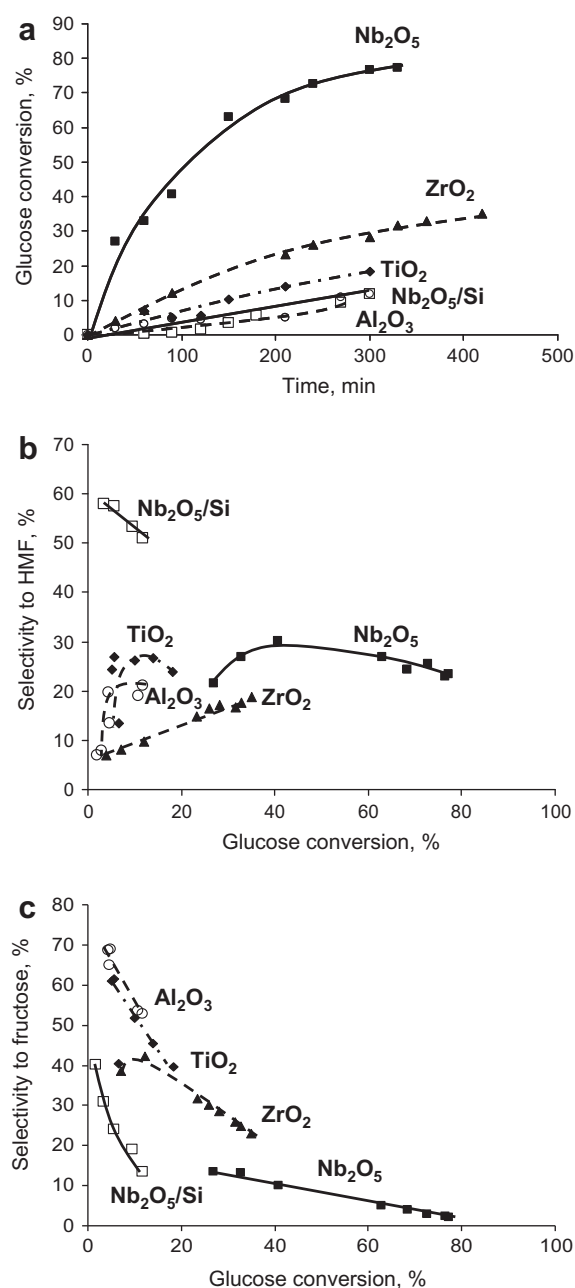


Fig. 7. Glucose conversion versus time (a), selectivity to HMF (b), and selectivity to fructose (c) versus glucose conversion over oxides.

transformed into humins, which cannot be observed by HPLC. To verify this and prove the formation of humins during the reaction, the products of the glucose dehydration over ZrPO after 6.5 h of the reaction were filtered. The solid part was dried and calcined at 600 °C. Calculation of the burned organic part as the product of glucose condensations shows that 29% of converted glucose was transformed into insoluble humins. At the same time, after 6.5 h of the reaction, 30% of glucose was transformed into HMF (26%), acids (3%), and fructose (1%). It means that about 40% of glucose should be in the form of soluble humins in the reaction mixture.

Unselective dehydration of glucose over Lewis acid sites might be shown by glucose dehydration over oxides (Fig. 7). The activity of glucose transformation over oxides decreases in the same order like over phosphate catalysts: $\text{Nb}_2\text{O}_5 > \text{ZrO}_2 > \text{TiO}_2 > \text{Al}_2\text{O}_3$ (Fig. 7a). This indicates that the activation of glucose molecules occurs

preferentially over the strong Lewis acid sites, the amount of which should decrease from Nb_2O_5 to Al_2O_3 . The selectivities to HMF over all oxide catalysts were in the range 10–30%, which confirms the hypothesis about unselective glucose dehydration over Lewis acid sites (Fig. 7b). It is interesting to note that the shape of the selectivity curves and their positions relative to each other over oxides resemble the selectivity curves to HMF during glucose dehydration over phosphates. This is a strong indication that oxide type Lewis acid sites play a role in the glucose dehydration over phosphates. In comparison with phosphates, glucose dehydration over oxides is accompanied by a more intensive glucose isomerization into fructose over Lewis acid sites (Fig. 7c). Thus, selectivities to fructose are 60–70% at low conversions even over aluminum and titanium oxides, which were inactive in isomerization in the form of phosphates. The selectivity decreases fast like over phosphates with an increase in the conversion of glucose due to subsequent fructose condensation into humins over Lewis acid sites.

These observations make clear the importance of the right combination of Brønsted and Lewis acidity in a catalyst for an effective glucose dehydration to HMF. In order to study this effect, we used modified Brønsted and Lewis acidity of zirconium and niobium phosphates.

3.2.2. Phosphates modification

The increase in the ratio Brønsted/Lewis (B/L) by modification of niobium and zirconium phosphates leads to significant changes in the catalytic properties (Fig. 5, Table 1). NbPO/Si and ZrPO/Si show an almost two times lower activity in comparison with the parent catalysts (Fig. 6). At the same time, the selectivity to HMF over NbPO/Si and ZrPO/Si increases to 60% and 55%, respectively. The silylation procedure leads mainly to deactivation of isolated Lewis acid sites from phosphate groups (Fig. 5). This observation indicates a high activity of isolated Lewis acid sites in the unselective glucose transformation into humins, which was shown by glucose dehydration over oxides (Fig. 7). A decrease in the amount of active Lewis acid sites leads to an increase in the selectivity of the process. Niobium phosphate on the basis of fresh niobic acid (NbPO-f) also shows a significantly lower activity in comparison with NbPO, but its activity is still higher than that of NbPO/Si. The selectivity over NbPO-f is 55% and comparable with the selectivity over NbPO/Si and ZrPO/Si. This is due to the high amount of phosphate groups in NbPO-f in comparison with NbPO, with a low amount of isolated Lewis acid sites leading to an unselective glucose transformation (Fig. 5). Hydroxyl groups in fresh niobic oxide are more active in interaction with phosphoric acid; however, these groups transform into stable Lewis acid sites in time. It is interesting to note that silylation of NbPO-f does not lead to changes in activity or selectivity of the catalyst (not shown), which means that already a low amount of isolated Lewis acid sites is present in this sample.

The poisoning effect of silylation over isolated Lewis acid sites can be shown over oxide catalysts. Most part of Lewis acid sites in the case of oxide should be formed by coordinatively unsaturated metal ions subjected to deactivation by a silylation procedure. Indeed, the treatment of niobic acid with TEOS leads to an almost complete deactivation of the catalyst (Fig. 7a). The performance of the silylated catalyst significantly differs from the parent oxide. It dehydrates glucose to HMF with a much higher selectivity (Fig. 7b). The strong Brønsted acid sites of niobic acid formed by hydroxyls [38] are apparently not deactivated by TEOS resulting in a high selectivity to HMF over the silylated catalyst.

The high slope of the line of the HMF selectivity for NbPO-f, ZrPO/Si, and NbPO/Si with an increase in glucose conversion indicates significant side reactions involving HMF. Indeed, Fig. 6c shows that the rate of acids formation increased significantly for modified catalysts. Thus, for NbPO-f, the selectivity to acids increases to 8%, in comparison with 2% over NbPO at a glucose

conversion of 40%. HMF transforms over Lewis acid sites mainly into humins, in comparison with the rehydration reaction to formic and levulinic acids, which proceeds over Brønsted acid sites [34]. Deactivation of isolated Lewis acid sites leads to an increase in the contribution of the rehydration reaction with an increase in the selectivity to acids. As expected, the suppression of the activity of Lewis acid sites in the catalysts leads to a significant decrease in the isomerization activity of glucose to fructose (Fig. 6d). The curves of the selectivity to fructose for NbPO-f, ZrPO/Si, and NbPO/Si have the same form like those for the parent catalysts, but they are shifted in the direction of lower conversions of glucose. The higher isomerization activity of ZrPO and NbPO over Lewis acid sites is supported by results of fructose and glucose adsorption (Table 1). A strong adsorption of sugars on NbPO and ZrPO is the result of the multiple interactions between strong Lewis acid sites and hydroxyl groups of sugars. These interactions lead to further isomerization of sugars [39]. It is interesting to note that the adsorption of fructose is almost 10 times higher over phosphates in comparison with glucose. The suppression of the Lewis acidity of phosphates ZrPO and NbPO after modification might be observed also from a decrease in sugars adsorption by two times for ZrPO/Si and NbPO-f (Table 1).

Thus, the modification of zirconium and niobium phosphates with a decrease in the contribution of Lewis acid sites leads to an increase in the selectivity of HMF formation. Indeed, the selectivity to HMF at 20% conversion of glucose depends on the ratio of B/L acid sites determined by Py adsorption and shows a gradual increase, indicating the strong influence of the composition of Brønsted and Lewis acid sites (Fig. 8). The decrease in the selectivity over catalysts with high Lewis acidity is the result of unselective glucose and fructose condensation into humins over isolated Lewis acid sites. The highest selectivity observed over NbPO-f corresponds to an equal amount of Lewis and Brønsted acid sites due to Nb—O—P centers.

In order to confirm this hypothesis and to study the role of both types of acid sites in glucose dehydration over phosphates, Na-exchanged samples were used. Na-exchanged samples possess only Lewis acidity and thereby give the opportunity to separate the process of glucose dehydration in two stages.

3.2.3. Dehydration of sugars over Na-exchanged phosphates

Fig. 9 shows a comparison of the fructose and glucose dehydration over NbPO before and after the exchange with Na. The glucose transformation over Na—NbPO has an almost two times higher

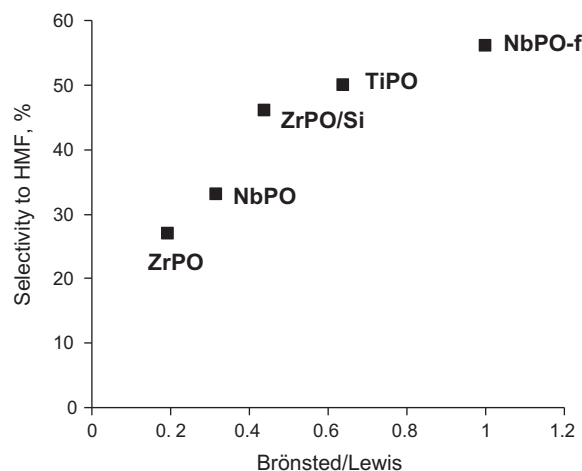


Fig. 8. Selectivity to HMF versus Brønsted/Lewis ratio determined by Py adsorption at 20% conversion of glucose.

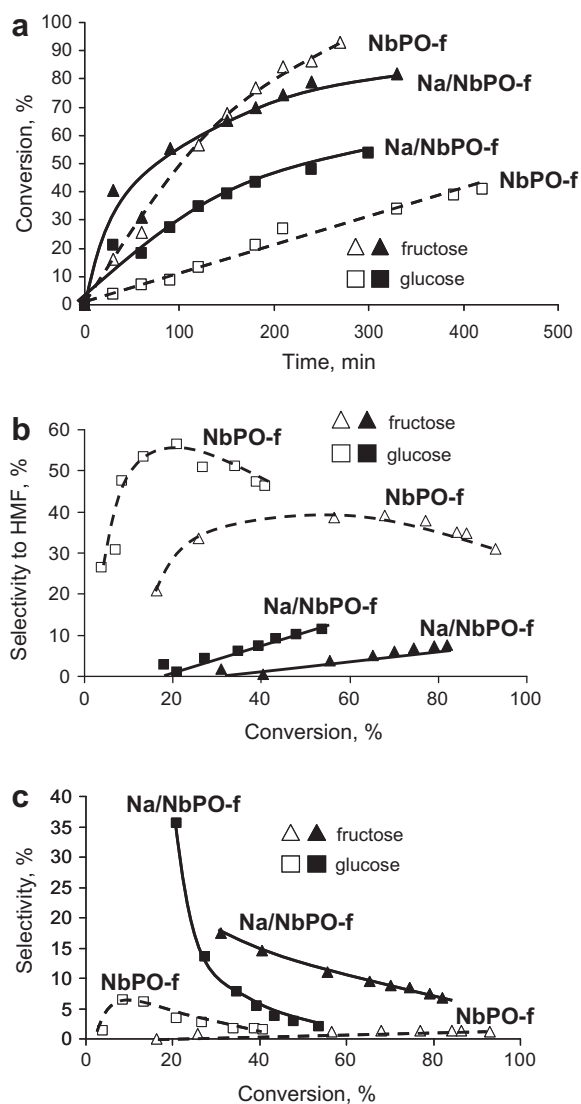


Fig. 9. Glucose and fructose conversion versus time (a), selectivity to HMF (b), and fructose or glucose (c) versus glucose or fructose conversion over parent NbPO and after ion exchange with Na.

activity in comparison with the parent NbPO (Fig. 9a). The main process over Na–NbPO is glucose isomerization to fructose instead of dehydration to HMF over NbPO (Fig. 9c). Thus, the selectivity to fructose decreases from 35% with increase in glucose conversion until almost full disappearance of it due to subsequent transformation into humins. At the same time, the selectivity to HMF increases with an increase in the glucose conversion to 10% (Fig. 9b), which might be due to the unselective fructose dehydration over Lewis acid sites [34]. Ion exchange of sodium cations with protons of formic and levulinic acids also might be the reason of fructose dehydration to HMF. However, the selectivity to acids

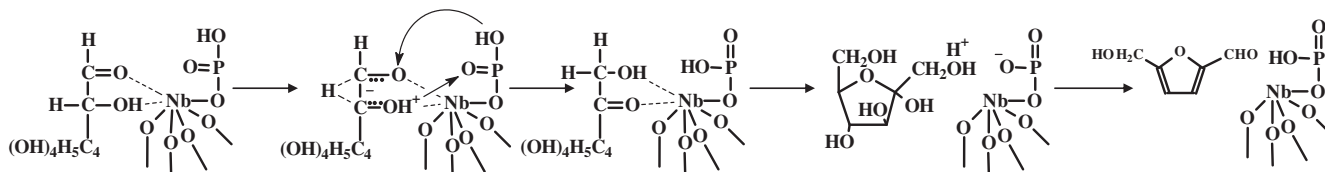
was very low (less than 2%) due to the low amount of HMF available for the rehydration reaction in the system and therefore they could lead only to partial exchange. At the same time, formation of HMF over an oxide catalyst (Fig. 7) shows that HMF might form over Lewis acid sites next to the main reactions of glucose isomerization to fructose and the condensation of sugars into humins.

It is interesting to note that the presence of protonated phosphate groups significantly suppresses the activity of Lewis acid sites in glucose transformation. A study of the acidity of NbPO-f indicates the close arrangement of Brønsted and Lewis acid sites in this sample (Fig. 5). Isomerization of glucose molecules into fructose over Lewis acid sites formed by Nb might be accompanied by subsequent dehydration over protonated phosphate groups without intermediate desorption of fructose molecules. This process can be described by Scheme 2. Protonated phosphate group might take part in the glucose isomerization by transfer of a proton between the oxygen of the first and second carbon. This will lead to a decrease in the accessibility of the Lewis acid site for the transformation of another molecule of glucose and thereby a lower activity. At the same time, it should result in a more efficient transformation of glucose into HMF due to the absence of an intermediate desorption of fructose from the Lewis acid site and a possible transformation into humins over another Lewis acid site.

The presence of isolated Lewis acid sites in the sodium exchanged catalyst should lead to a lower or comparable activity in glucose transformation in comparison with the parent sample. Indeed, testing of the catalyst ZrPO with a high isolated Lewis acidity shows a comparable activity in the glucose transformation before and after ion exchange with Na⁺ (Fig. 10).

The fructose transformation over NbPO and Na–NbPO catalysts occurs with similar activities, which is much higher than the activity in glucose dehydration over NbPO and Na–NbPO catalysts (Fig. 9a). This indicates a higher reactivity of the fructose molecule both over Brønsted and over Lewis acid sites in comparison with glucose due to the furanose ring structure. Fructose transforms over Lewis acid sites of Na–NbPO mainly into humins and glucose (Fig. 9). The selectivity to glucose over Na–NbPO is even higher than the isomerization of glucose into fructose, what might be explained by a lower rate of consecutive glucose transformation.

The activity of Na–NbPO in the fructose dehydration to HMF, similar to the case of glucose, is also very low and the selectivity to HMF does not exceed 10%. It is interesting to note that the selectivity of fructose dehydration over NbPO to HMF is lower in comparison with the glucose dehydration to HMF. The maximum selectivity of fructose dehydration to HMF over NbPO-f was only 40%, whereas over NbPO-f glucose dehydrates to HMF with a maximum selectivity of 55%. The low selectivity to HMF during fructose dehydration is the result of a separate unselective fructose transformation over a Lewis site and nearby phosphate group. Glucose seems to be more stable to condensation into humins over protonated phosphate groups. The adsorption of glucose on Lewis acid site with subsequent isomerization and further dehydration over nearby phosphate group results in a higher selectivity of the process (Scheme 2). It is interesting to note that glucose and fructose dehydration proceeds with similar selectivities (30%) over zirconium phosphate (Fig. 10). This is the result of separate stages of



Scheme 2.

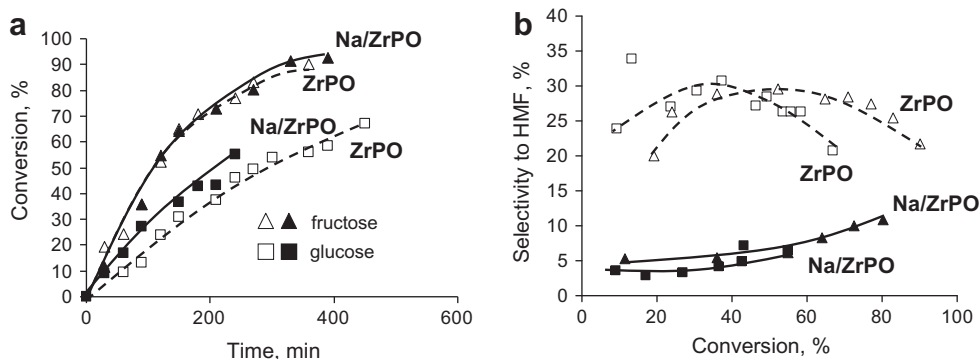


Fig. 10. Glucose and fructose conversion versus time (a) and selectivity to HMF versus glucose or fructose conversion (b) over parent ZrPO and after ion exchange with Na.

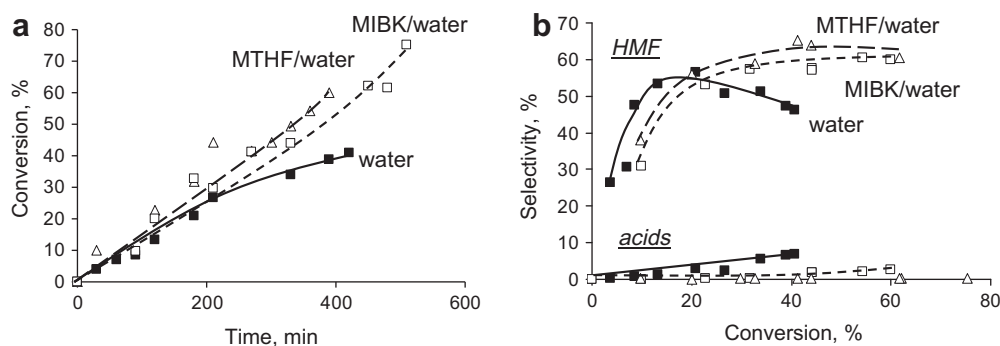


Fig. 11. Glucose conversion versus time (a) and selectivity to HMF and acids (b) versus glucose conversion over NbPO-f in aqueous phase and with addition of 3 vol. of MIBK or MTHF.

glucose isomerization over Lewis acid sites with subsequent desorption and dehydration or condensation over other Lewis acid sites or phosphate groups.

Thus, the synergism in the two-stage process results in a higher selectivity of glucose dehydration into HMF. However, at high conversions of glucose the selectivity to HMF starts to decrease due to the secondary processes of HMF rehydration and condensation with sugars into humins. It was shown earlier that the addition of organic solvents absorbing HMF leads to a suppression of the side reactions of HMF transformation [34,40].

3.2.4. Glucose dehydration in biphasic system

Fig. 11 shows a comparison of glucose dehydration over NbPO-f without and in the presence of organic solvents like MIBK and MTHF. The activity of the catalyst is comparable at low conversion of glucose, although addition of organic solvents leads to an increased activity at high conversions of glucose. This fact is the result of the deactivation of the catalyst during the reaction in water by humins deposition on the surface of the catalyst. Extraction of HMF and humins by MIBK and MTHF, which is visible by a clearing of aqueous phase and a darkening of the organic phase, suppresses the deactivation of the catalyst (Fig. 11).

Extraction ratios of HMF for MIBK and MTHF are 0.9 and 1.5, respectively. This means that the addition of three volumes of organic solvent leads to a decrease in the concentration of HMF in aqueous phase by factor of 3.6 and 6 for MIBK and MTHF, respectively. This decrease in the concentration of HMF in the aqueous phase leads to a decrease in the amount of formed acids in the reaction mixture (Fig. 11). Thus, without an addition of organic solvents, the selectivity to acids is 7% at 40% glucose conversion and the addition of MIBK and MTHF leads to a decrease in the selectivity to 1.78% and 0.3%, respectively. At the same time, the addition

of organic solvents leads to a stabilization of the selectivity to HMF at about 60%. In comparison with the significant beneficial effect of the addition of organic solvents on the selectivity to HMF during dehydration of fructose, absorption of HMF during glucose dehydration leads only to a preservation of the maximum selectivity to HMF [34]. This is a result of the significantly higher rate of secondary HMF rehydration to acids and HMF condensation with fructose over Brønsted acidic systems [34]. The addition of solvent in this case results in a larger effect on the selectivity.

Thus, the presence of organic solvents during the glucose dehydration over phosphates leads to a suppression of the deactivation of the catalyst and stabilizes the selectivity to HMF at high conversions of glucose.

4. Conclusions

The investigation of the acidic properties of phosphates of Al, Ti, Nb, and Zr suggests that the amount of strong Brønsted acid sites increases in accordance with the decrease in electronegativity of the metals. Lewis acidity in phosphates consists of metal sites bound to phosphate groups and isolated Lewis acid sites. Treatment of phosphates of Nb and Zr with TEOS allows us to decrease the amount of isolated Lewis acid sites.

Phosphates of aluminum, zirconium, and niobium are shown to be effective catalysts for glucose dehydration to HMF. The conversion of glucose over phosphates increases in the following order: AlPO < TiP < ZrP < NbP in accordance with increase in the strength of acid sites. The selectivity to HMF increases with the increase in the ratio of Brønsted to Lewis acid sites with a decrease in the amount of isolated Lewis acidity. The highest selectivity to HMF is found to be 55–60% over silylated phosphates.

The selective elimination of Brønsted acidity by Na treatment shows the synergism of nearby Lewis and Brønsted acid sites in the two-stage process of glucose transformation into HMF. It leads to a higher selectivity to HMF in comparison with a separate glucose isomerization over Lewis acid sites and fructose dehydration to HMF over phosphate groups.

The addition of organic solvents like MIBK and MTHF leads to a higher activity of the catalyst and suppression of HMF rehydration in acids and condensation into humins with stabilization of the selectivity to HMF on the level of the maximum selectivity during the aqueous phase dehydration.

Acknowledgments

This research is being performed within the framework of the CatchBio program (053.70.001). The authors gratefully acknowledge the support of the Smart Mix Program of the Netherlands Ministry of Economic Affairs and the Netherlands Ministry of Education, Culture and Science.

References

- [1] X. Tong, Y. Ma, Y. Li, *Appl. Catal. A* 385 (2010) 1.
- [2] A. Corma, S. Iborra, A. Velty, *Chem. Rev.* 107 (2007) 2411.
- [3] B.F.M. Kuster, L.M. Tebbens, *Carbohydr. Res.* 54 (1977) 159.
- [4] Y. Nakamura, S. Morikawa, *Bull. Chem. Soc. Jpn.* 53 (1980) 3705.
- [5] Y. Román-Leshkov, J.N. Chheda, J.A. Dumesic, *Science* 312 (2006) 1933.
- [6] C. Lansalot-Matras, C. Moreau, *Catal. Commun.* 4 (2003) 517.
- [7] L. Hu, Y. Sun, L. Lin, *Ind. Eng. Chem. Res.* 51 (2012) 1099.
- [8] Z. Yuan, C. Xu, S. Cheng, M. Leitch, *Carbohydr. Res.* 346 (2011) 2019.
- [9] M. Ohara, A. Takagaki, S. Nishimura, K. Ebitani, *Appl. Catal. A* 383 (2010) 149.
- [10] M. Watanabe, Y. Aizawa, T. Iida, R. Nishimura, H. Inomata, *Appl. Catal. A* 195 (2005) 195.
- [11] H.P. Yan, Y. Yang, D.M. Tong, X. Xiang, C.W. Hu, *Catal. Commun.* 10 (2009) 1558.
- [12] F. Yang, Q. Liu, X. Bai, Y. Du, *Bioresour. Technol.* 102 (2011) 3424.
- [13] F. Yang, Q. Liu, M. Yue, X. Bai, Y. Du, *Chem. Commun.* 47 (2011) 4469.
- [14] G. Hutchings, I. Hudson, D. Timm, *Catal. Lett.* 61 (1999) 219.
- [15] S.M. Patel, U.V. Chudasama, P.A. Ganeshpure, *Green Chem.* 3 (2001) 143.
- [16] V.F.D. Alvaro, R.A.W. Johnstone, *J. Mol. Catal. A: Chem.* 280 (2008) 131.
- [17] S. Okazaki, A. Kurosaki, *Catal. Today* 9 (1990) 113.
- [18] M. Xuebing, F. Xiangkai, *J. Mol. Catal. A: Chem.* 208 (2004) 129.
- [19] T. Armaroli, G. Busca, C. Carlini, M. Giuttari, A.R. Galletti, G. Sbrana, *J. Mol. Catal. A: Chem.* 151 (2000) 233.
- [20] D. Prasetyoko, Z. Ramli, S. Endud, H. Nur, *Mater. Chem. Phys.* 93 (2005) 443.
- [21] M.J. Hudson, A.D. Workman, R.J.W. Adams, *Solid State Ionics* 46 (1991) 159.
- [22] A. Sinhamahapatra, N. Sutradhar, B. Roy, A. Tarafdar, H.C. Bajaj, A.B. Panda, *Appl. Catal. A* 385 (2010) 22.
- [23] K. Segawa, Y. Nakajima, *J. Catal.* 101 (1986) 81.
- [24] L.C. Jozefowicz, H.G. Karge, E.N. Coker, *J. Phys. Chem.* 98 (1994) 8053.
- [25] M.C. Kung, H.H. Kung, *Catal. Rev. Sci. Eng.* 27 (1985) 425.
- [26] B.A. Morrow, I.A. Cody, *J. Phys. Chem.* 80 (1976) 1995.
- [27] H. Miyata, J.B. Moffat, *J. Catal.* 62 (1980) 357.
- [28] S. Zheng, H.R. Heydenrych, A. Jentys, J.A. Lercher, *J. Phys. Chem. B* 106 (2002) 9552.
- [29] D. Spielbauer, G.A.H. Mekhemer, T. Riemer, M.I. Zaki, H. Knozinger, *J. Phys. Chem. B* 101 (1997) 4681.
- [30] G.A.M. Hussein, N. Sheppard, M.I. Zaki, R.B. Fahim, *J. Chem. Soc. Faraday Trans.* 85 (1989) 1723.
- [31] S. Li, A. Zheng, Y. Su, H. Zhang, L. Chen, J. Yang, C. Ye, F. Deng, *JACS* 129 (2007) 11161.
- [32] D.A. Nelson, P.M. Molton, J.A. Russell, R.T. Hallon, *Ind. Eng. Chem. Prod. Res. Dev.* 23 (1984) 471.
- [33] B.F.M. Kuster, *Carbohydr. Res.* 54 (1977) 177.
- [34] V.V. Ordonsky, J. van der Schaaf, J.C. Schouten, T.A. Nijhuis, *ChemSusChem* 5 (2012) 1812.
- [35] V.L. Sushkevich, V.V. Ordonsky, I.I. Ivanova, *Appl. Catal. A* 441–442 (2012) 21.
- [36] M. Moliner, Y. Roman-Leshkov, M.E. Davis, *PNAS* 107 (2010) 6164.
- [37] Y. Zhang, E.A. Pidko, E.J.M. Hensen, *Chem. Eur. J.* 17 (2011) 5281.
- [38] K. Tanabe, *Mater. Chem. Phys.* 17 (1987) 217.
- [39] M. Moliner, Yu. Román-Leshkov, M.E. Davis, *PANS* 107 (2010) 6164.
- [40] V.V. Ordonsky, J. van der Schaaf, J.C. Schouten, T.A. Nijhuis, *J. Catal.* 287 (2012) 68.